JMEPEG (2012) 21:797–808
DOI: 10.1007/s11665-011-9964-6

1059-9495/$19.00

Prediction of Tool Wear Mechanisms in Face Milling AISI 1045 Steel

Patricia Muñoz-Escalona, Nayarit Díaz, and Zulay Cassier

(Submitted June 8, 2010; in revised form April 5, 2011)

Cutting tools have an important role in the machining process, since they are related to workpiece surface quality and production costs. Due to the importance of selecting appropriate cutting parameters during the milling process, this research develops empirical expressions to predict the tool wear mechanisms that a cutting tool will suffer during the milling of AISI 1045. In addition, an expression to predict the critical cutting speed value where the diffusion mechanism starts to appear is developed. AISI 1045 was selected as the workpiece material due to its excellent machinability, good abrasion resistance, and mechanical strength. The Design of Experiments method namely Taguchi was applied to reduce the time and cost of experiments. The results showed that the cutting speed is the parameter with the most influence on tool flank wear which started to appear when using V = 500 m/min and the diffusion tool wear mechanism at V = 850 m/min.

Keywords cutting speed, Taguchi, tool wear, wear mechanism

1. Introduction

Tool wear is related to all the cutting tools involved in a machining process, and once a tool is past its wear limit it diminishes workpiece quality. The cutting tool is influenced by different tool wear mechanisms such as: abrasion, diffusion, oxidation, fatigue, and adhesion. These mechanisms degrade the cutting tool to a final stage where the tool reaches the end of its life.

It is very important to predict the level of tool wear generated on the tool, to optimize the machining process. Many researchers have focused their efforts in tool wear studies, concluding that the cutting speed, feed, and the depth of cut are the parameters with most influence on this phenomenon.

2. Literature Review of Tool Wear Evaluation

This review of tool wear literature is divided into three major categories which relate to the research areas carried out by the authors, together with a brief critique and identification of the research gap which the research in this article addresses. These three categories consist of:

(i) Tool wear evaluation via empirical experimental machining.
(ii) Tool wear evaluation via mathematical models.
(iii) The application of Taguchi in tool wear evaluation.

Patricia Muñoz-Escalona, Nayarit Díaz, and **Zulay Cassier**, Universidad Simón Bolívar, Mecánica, Edf. Meu. 3er Piso. Valle de Sartenejas, Caracas 1080, Venezuela. Contact e-mail: pmunoz@usb.ve.

2.1 Tool Wear Evaluation via Empirical Experimental Machining

In 1997, Elbestawi et al. (Ref 1) performed some experiments using several grades of polycrystalline cubic boron Nitride (PCBN) ball-nose end mills with various types of edge for the high-speed milling of H13 tool steel. They concluded that the higher contents of cubic boron nitride (CBN) (90%) on PCBN tools are recommended for milling hardened tool steel and that the main mode of tool failure was classical flank wear.

Koshy et al. (Ref 2) in 2002 machined AISI D2 (HRC = 58), using solid carbide ball-nose end mills and indexable inserts employing carbide and cermets tools. They concluded that chipping, adhesion, and attrition were, in general, the governing mechanisms responsible for tool wear and that PCBN tools failed by fracture of the cutting edge. However, a better surface roughness was obtained with PCBN end mills. Tool wear mechanisms of a HSS cutting tool were also studied by Hogmark (Ref 3). They concluded that it is usual to find the presence of two wear mechanisms on the cutting tool and that the abrasive tool wear can be classified as medium and severe. At high cutting speeds, the generation of temperature in the workpiece surface-cutting tool interface is increased, easing a strong adhesion between them. The tool strain is a consequence of a combination between cutting forces and temperatures due to the increase of the cutting speed during the machining process. The fatigue tool wear mechanism is generated due to an increase of the cutting speed during the machining process, and is produced due to intermittent cutting especially when combining high cutting speeds and the machining of a hard and ductile material.

In 2002, Liu et al. (Ref 4) studied the wear patterns and mechanisms of cutting tools during high-speed face milling of different working materials such as: cast iron, 45# tempered carbon steel, and 45# hardened carbon steel. They demonstrated that lower CBN content in the PCBN tool is not suitable for the high-speed machining of steels with hardness less than 45 to 50 HRC and that it is necessary to select a higher CBN content PCBN tool (more than 90% CBN) in intermittent high-speed milling operations.

With regards the effect of the built up edge phenomenon on the tool wear, this was studied by Cassier (Ref 5). The studies were focused on the effect of this phenomenon on coated and uncoated carbides during the turning of AISI 1020, AISI 1045, and AISI 4140 at low cutting speeds. The results showed that the abrasion and adhesion mechanisms are responsible for tool flank wear when using uncoated carbide tools, while coated tools were affected only by the abrasive mechanism. Also, they concluded that the feed rate is the cutting parameter with most influence on the tool flank wear when turning at low cutting speed.

Devillez et al. (Ref 6) studied the tool wear mechanisms when turning 42CrMo4. Their studies concluded that premature tool failure is caused by the abrasion, the adhesion, and the diffusion mechanisms, where the diffusion and abrasion mechanism produced the presence of a crater on the tool flank edge. In addition, the results showed that the abrasion mechanism is present at low cutting speeds.

The influence of the cutting parameters on the tool wear during a machining process has also been a major study area over recent years. Serdar et al. (Ref 7) analyzed the behavior of three types of milling cutter to study the effect of the cutting speed on tool wear when using a constant feed rate. They showed that tool flank wear increased when cutting speed was increased. This was determined using an optical microscope, while the tool wear mechanisms were analyzed using electron microscope. De Melo et al. (Ref 8) studied tool life by studying the tool wear mechanisms and tool damage such as fracture, chipping, and thermal fatigue on cement carbide tools during milling. Their studies showed that tool wear is inevitable, and that the presence of fissures in the cutting edge is due to the thermal and mechanical fatigue mechanism and due to the spindle speed. This is due to the tool being constantly exposed to mechanical shocks and thermal changes, which is a characteristic of milling.

The tool wear mechanisms in coated carbide tools were studied by Bahn et al. (Ref 9) when machining AISI 1045. The tool life criterion was based on the tool flank wear, since this is the main mechanism related to tool life. They concluded that the high temperatures and forces generated during the cutting process are the main reason of tool failure when machining at high cutting speed and feed rates.

2.2 Tool Wear Evaluation via Mathematical Models

Regarding statistical models for tool wear, Molinari and Nouari (Ref 10) developed two theoretical models for the prediction of diffusion wear when machining at high cutting speeds. The first model is governed by the cutting temperature and the second model explains the non-uniform distribution of the temperature at the tool-chip interface. The studies revealed that the diffusion mechanism is presented when using high cutting speeds, due to the increase of the temperature between the chip and the cutting tool interface. Another mathematical model for tool wear prediction was developed by Choudhury and Srinivas (Ref 11). The model was based on the cutting parameters during the turning process. The selected cutting parameters were: cutting speed, feed, depth of cut, tool hardness, and the diffusion coefficient. The results showed that the cutting speed and the diffusion coefficient are the factors which most affect the tool flank wear, followed by the feed and the depth of cut. That same year Korkut et al. (Ref 12), studied the influence of cutting speed on tool wear and surface roughness when turning AISI 304 austenitic stainless steel. The results showed a decrease in tool wear when increasing the cutting speed up to 180 m/min while a decrease in surface roughness was found with an increase in the cutting speed.

2.3 The Application of Taguchi in Tool Wear Evaluation

With the idea of involving a larger variety of cutting parameters and optimizing the number of experiments to be conducted, a few researchers have applied the Taguchi Method in their tool wear studies. In 2009, Gopalsamy et al. (Ref 13) developed equations for the prediction of tool wear and surface roughness. The equations were based on a multiple regression analysis. The experiments were conducted on hardened steel when using an end milling process. As Design of Experiments the Taguchi method was applied, the signal-to-noise ratio and analysis of variance (ANOVA) were applied to study the performance of the cutting speed, feed, and depth of cut, on the machined surface finish and the tool life. The results showed that cutting speed is the most influential parameter and that chipping and adhesion were the main causes of tool wear. It was also observed that the Taguchi method matched closely with the ANOVA results.

Calamaz et al. (Ref 14) studied tungsten carbide (WC-Co) tool wear under dry machining of the hard-to-cut titanium alloy Ti6Al4V. Machining tests were conducted in an orthogonal cutting framework and showed a strong evolution of the cutting forces and chip profiles with tool wear. The wear mechanisms were identified using cutting force measurements, scanning electron microscope observations, and optical profilometer analysis. The results showed that the chip formation mechanisms during the cutting process are quite dependent of the worn tool geometry. Also in 2009, Rashed and Makmoud (Ref 15) predicted tool wear based on an artificial neural network (ANN) approach. The studies were conducted to predict and optimize the wear rates on A356/SiC metal matrix composites (MMCs).

2.4 Critique and Research Gap

As observed from above, few researchers have focused their studies on the influence of cutting parameters on the tool wear. Other researchers have studied the effect that the cutting parameters produce on the diffusion tool wear mechanisms and others have studied the tool wear phenomenon based on statistical and engineer methods such as the Taguchi method for the optimization of time and cost of experiments. In general, all the researchers agree that the cutting speed has an important influence on the tool life, since depending on its value the tool is influenced by one or more tool wear mechanisms. Also there are different mathematical models related to tool wear prediction, however, they are not related to the tool wear mechanism. In this article, to make a new contribution to knowledge the intention of this research is to develop an empirical expression for the prediction of tool flank wear for different tool wear mechanisms when face milling AISI 1045 and an empirical expression for the prediction of the critical cutting speed, which is the speed when tool wear changes from mechanical wear to thermal wear. These expressions represent a useful tool for manufacturing industries since it will allow the selection of optimal combinations of cutting parameters for best tool performance as well as the possibility of reaching a better control of the final workpiece surface quality, tool life, and a reduction in costs and production time.

Table 1 Chemical composition of AISI 1045

%C	%Si	%Mn	%P	%S
±0,0001 0.4881	±0,0001 0.2574	±0,0001 0.7260	±0,0001 0.0235	±0,0001 0.0260

Table 2 Mechanical properties of AISI1045

Ultimate strength, MPa	743
Brinell hardness (a)	234

(a) Load = 3000 kg and $Ø_{ball}$ = 10 mm

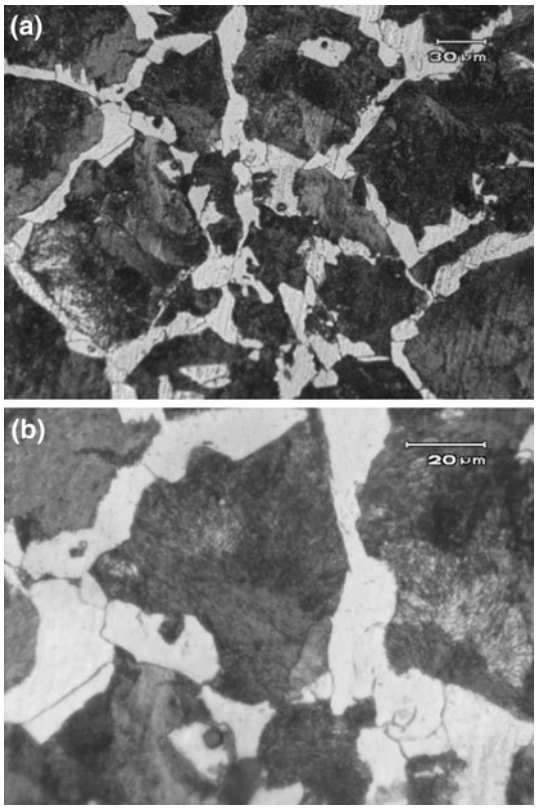

Fig. 1 AISI 1045 original microstructure. (a) 200× and (b) 400×

3. Experimental Procedure

3.1 Workpiece Characteristics

AISI 1045 round bars with the following geometry Ø = 76.2 mm and L = 165 mm were used. These round bars were premachined into a square shape bar of 165 x 70 × 30 mm as suggested by ISO 8688-1. Table 1 shows the chemical composition and Table 2 the mechanical properties of the AISI 1045.

Metallographic techniques were conducted following the ASTM E3 standards to reveal the original microstructure of this AISI 1045 carbon steel. Figure 1 shows the AISI 1045 original microstructure, where a perlitic phase (dark zone) and a ferritic phase (white zone) can be observed. As expected the dark zone is larger than the white zone due to the amount of carbon presented in this steel.

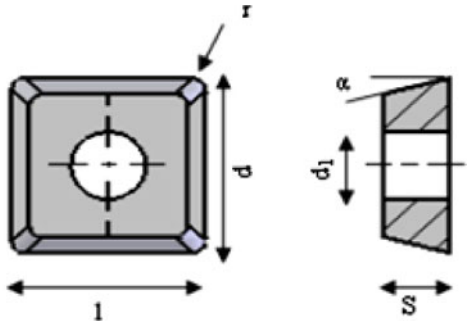

l (mm)	d (mm)	S (mm)	r (mm)
50	40	14	0.8

Fig. 2 Geometry of the inserts used for the machining experiments

3.2 Tool and Tip Characteristics

A face mill cutting tool with a standard insert holder of Ø = 50 mm, with six cutting teeth, was used for the experiments. Indexable SONX coated tungsten carbide inserts, model 150508TR-M14 (CVD-T250), were selected for the study. This type of insert is recommended by the tool manufacturer for optimal machining cuts when using AISI 1045 as the workpiece. Figure 2 shows the cutter and inserts dimensions.

3.3 Cutting Parameters

The cutting parameters selected for this study were the cutting speed, the feed per tooth, and the depth of cut, since from the limited previous research it was observed that these variables had most influence on the tool wear mechanisms during the machining process (Ref 3, 4, 6-10). Selected cutting parameters are shown in Table 3.

Twelve levels were selected for the cutting speed to warranty the presence of different tool wear mechanisms, three levels for the feed per tooth and the axial depth of cut.

3.4 Equipment Characteristics

A FADAL CNC milling equipment, model VMC 3016, with a maximum spindle of 10.000 rpm was used for the face milling operation. All the experiments were conducted under a dry cutting environment.

3.5 Design of Experiments: Taguchi Method

For the Design of Experiments the Taguchi Method was applied. For the selection of the orthogonal array, the experiments were divided into two groups. Each group consists of six levels of cutting speed, three levels of feed per tooth, and three levels for the axial depth of cut. This was due to select the orthogonal arrays suggested by the Minitab 14 software. The selected orthogonal array corresponds to a L_{18} ($6^1 \times 3^2$), which corresponds to one factor with six levels and two factors with three levels each. This array gives a total of 18 trials for each group. For the second group, the same orthogonal array was used but using the other six levels of the cutting speed. Table 4 shows the orthogonal array employed for this study.

The numerical values for each level and each group are shown in Table 5.

Table 3 Selected cutting parameters

	Levels											
Factors	**1**	**2**	**3**	**4**	**5**	**6**	**7**	**8**	**9**	**10**	**11**	**12**
V, m/min	150	250	350	450	550	650	750	850	950	1050	1150	1250
fz, mm/rev · tooth	0.1	0.2	0.3	…	…	…	…	…	…	…	…	…
ap, mm	2.5	3.5	4.0	…	…	…	…	…	…	…	…	…

Table 4 $L_{18}(6^1 \times 3^2)$ orthogonal array for the experiments

Trial	*V*, m/min	fz, mm/rev · tooth	ap, mm
1	1	1	1
2	1	2	2
3	1	3	3
4	2	1	1
5	2	2	2
6	2	3	3
7	3	1	2
8	3	2	3
9	3	3	1
10	4	1	3
11	4	2	1
12	4	3	2
13	5	1	2
14	5	2	3
15	5	3	1
16	6	1	3
17	6	2	1
18	6	3	2

Table 5 Selected values for each level for Groups 1 and 2

	Levels					
Factors	**1**	**2**	**3**	**4**	**5**	**6**
Group 1						
V, in/min	150	250	350	450	550	650
fz, min/rev · tooth	0.1	0.2	0.3			
ap, mm	2.5	3.5	4.0			
Group 2						
V, m/min	750	850	950	1050	1150	1250
fz, mm/rev · tooth	0.1	0.2	0.3			
ap, mm	2.5	3.5	4.0			

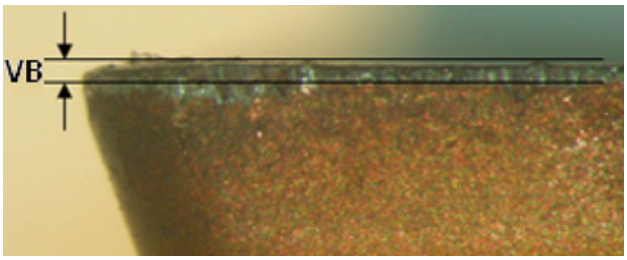

Fig. 3 Tool flank wear measurement, VB

3.6 Tool Life Criterion and Tool Wear Measurement

The most commonly used criterion to identify tool life is tool flank wear and to define a correct tool deterioration criterion, the ISO Standard 8688-1 (Ref 16) was followed. This standard is specific for face milling operations where different values of tool flank criteria are suggested. The maximum value of flank wear considered in this standard is VB = 0.5 mm, but to reduce the time of experiments the lowest numerical value of tool deterioration suggested by this standard was selected (VB = 0.2 mm). Once the insert reached this value, tool life has been reached, although if chipping or cracking was shown before a VB = 0.2 mm, then tool life will also considered as over.

It should be highlighted that for all the trials new inserts were used to ensure consistency of the tool wear and tool life results. Only the insert which presented the highest deterioration out of the six inserts was the one selected for the study. Tool wear was measured three times after each single pass (L = 165 mm) and ended once reaching a VB = 0.2 mm or a maximum of six passes (L = 995 mm). The trials were duplicated to assure the results and the average of each trial was reported as the tool flank wear result. The measurements were conducted using a PZO-MWM tool microscope with a resolution of ±0.1 mm and a magnification of de 15×. Each measurement was conducted three times to avoid any possible mistake during the procedure.

For the tool wear mechanism analysis, the tool flank wear evolution was observed using a magnifier and an electron scan microscope. Also the tool surface morphology was observed to identify the characteristics that define each type of tool wear mechanism. With regards the tool that presented evidence of adhesion and diffusion tool wear mechanisms an energy dispersive x-ray (EDX) analysis was conducted to assure the presence of these mechanisms in the affected surface.

Once tool wear results were obtained the empirical expressions for tool wear prediction were developed. These empirical expressions were obtained applying a multiple linear regression analysis using the Minitab 14 software. The dependent variable is tool wear where the main tool wear mechanism is presented (VB_{AB}: abrasion mechanism, VB_{AD}: adhesion mechanism, VB_D: diffusion mechanism, VB_{TF}: thermal fatigue mechanism, VB_{MF}: mechanical fatigue mechanism), and the independent variables: the cutting speed (V), the feed per tooth (fz), and the depth of cut (ap). Figure 3 shows the tool flank measurement, VB.

4. Results and Discussions

Once all the trials were conducted the following results were obtained. Figure 4 shows a few examples of tool wear when milling AISI 1045 under different cutting conditions.

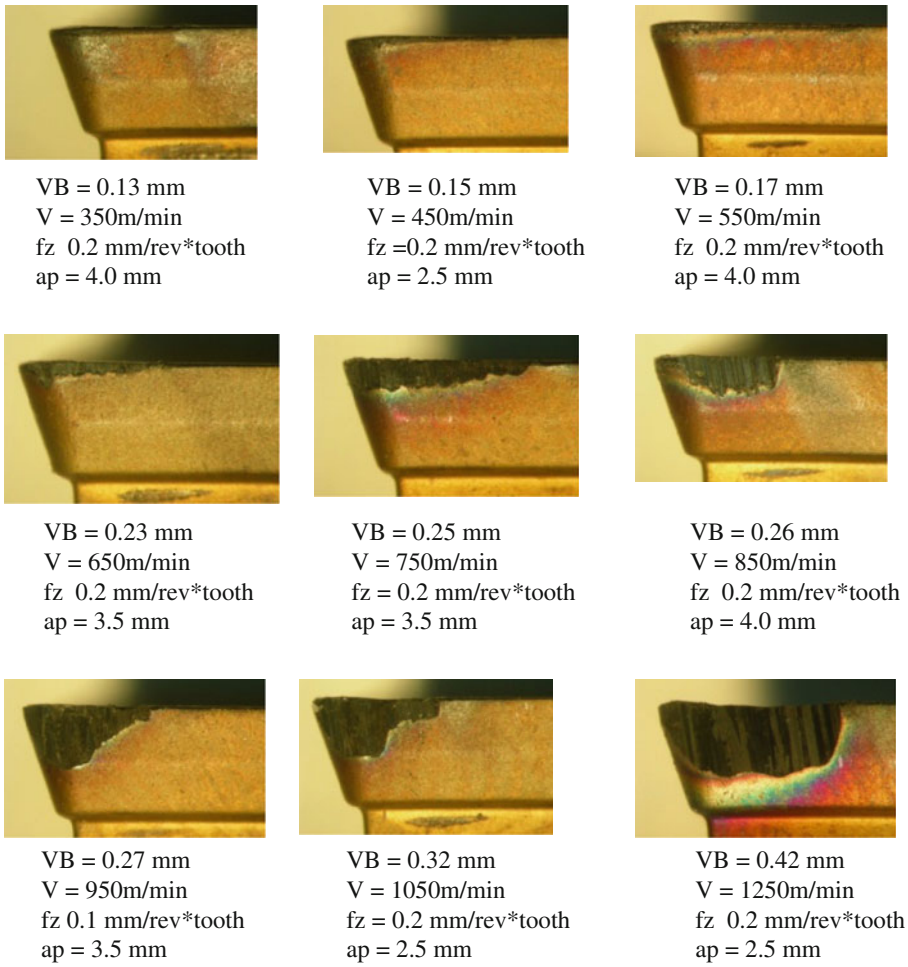

Fig. 4 Few examples of tool wear evolution when face milling AISI 1045 under different cutting conditions

It must be highlighted that in all cases tool flank wear started to appear when using $V = 500$ m/min and that different tool wear mechanisms appeared simultaneously in each of the different tool's surface when cut under different cutting conditions.

Figure 5(a) and (b) shows the scanning electron microscope (SEM) pictures of the tool surface for a new tool. These pictures will be used as the starting point for the tools that suffer tool wear during the milling process of the AISI 1045.

Figure 6 shows a tool's structural surface with a VB = 0.17 mm. This tool conducted a milling process when using $V = 450$ m/min, fz = 0.3 mm/rev · tooth, and ap = 3.5 mm. In this figure, it can be observed that the tool is affected by different tool wear mechanisms.

When analyzing Fig. 6(a) it can be observed that there is a presence of fissures located perpendicular to the cutting edge. These fissures were probably generated due to the temperature and loads the tool is involved into during the milling process. These fissures are characteristics of a worn tool involved in a thermal fatigue tool wear mechanism. Also from Fig. 6(a), it can be observed that the cutting tool lost some material, this is known as chipping. This chipping is perpendicular to the cutting edge and is a characteristic of a mechanical fatigue tool wear mechanism. The presence of chipping is due to cyclic loads, which is typical of intermittent cuts such as the milling process (Ref 8, 17).

In Fig. 6(b), the presence of lines in the cutting tool surface along the chip flow direction can be observed. These lines are produced due to the constant movement of hard particles that comes from the workpiece. The presence of these marks on the tool's surface is characteristic of the abrasion tool wear mechanism (Ref 3, 8, 17).

Figure 7 shows a tool's structural surface with VB = 0.3 mm. This tool was used for the face milling process of the AISI 1045 when cutting with $V = 950$ m/min, fz = 0.3 mm/rev · tooth, and ap = 2.5 mm.

When analyzing Fig. 7(a), the presence of the abrasion tool wear mechanism can be observed. In this same figure a crater can also be observed where the diffusion tool wear mechanism is presented. In order to corroborate this result, an EDX analysis was conducted in the gap located at the tool's crater (Fig. 7c). The results of this analysis show the presence of the chemical elements, C and Fe, which are elements that belong to the AISI 1045, as well as C and W which are the tool chemical elements. The result of this analysis is shown in Fig. 8. Also in Fig. 7(a) and (b), the presence of adhered particles on the tool's surface can be observed. These particles come from the milled material and corroborate the presence of the adhesion tool wear mechanism.

In order to select the optimal combination of cutting parameters for the minimum tool wear for an specific tool wear mechanism, the statistical measure of performance, called

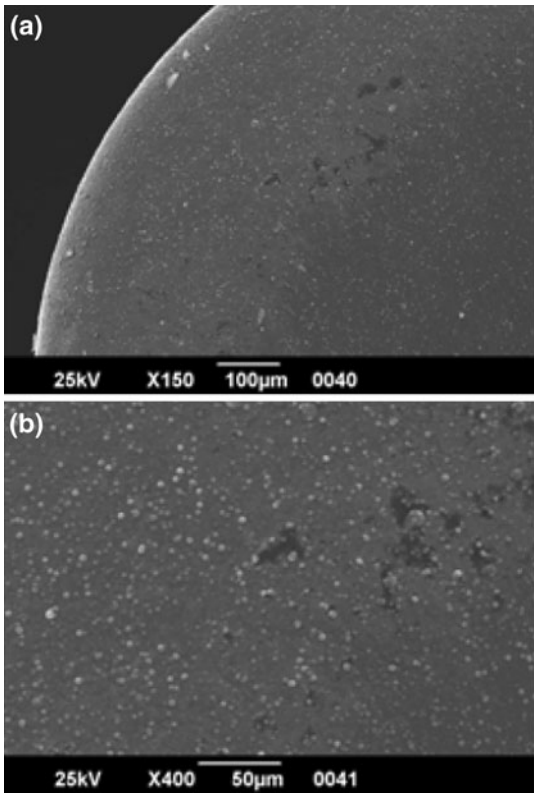

Fig. 5 SEM pictures of a new tool. (a) 150× and (b) 400×

signal-to-noise ratio (S/N), developed by Taguchi was applied. This measure also allowed the identification of the optimal combination of cutting parameters for a specific objective, which in this case study corresponds to the smallest tool wear for a longer tool life. For this analysis, the S/N ratio, smaller-the-best formula was applied. In Fig. 9, the S/N ratio for different tool wear mechanisms is presented: S/N VB_{AB}, S/N VB_{AD}, S/N VB_{D}, S/N VB_{TF}, S/N VB_{MF}.

When analyzing Fig. 9, it can be observed that few trial presented different tool wear mechanisms simultaneously. Also, as observed in this figure, the highest S/N VB_{AB} (which represents the smallest amount of abrasion tool wear mechanism) is presented in trial 4, which used V = 250 m/min, fz = 0.1 mm/rev · tooth, and ap = 2.5 mm. This trial 4 was conducted with the lowest levels of cutting parameters. This result is due to the fact that the chip cross-sectional area is small since low values of fz and ap are used. This produces less friction against the cutting tool surface and the cutting forces decrease producing less wear on the tool's surface (Ref 4, 7). With regard to the adhesion tool wear mechanism, as observed, trial 19 cutting parameter combination produces less tool wear. This trial was conducted at V = 750 m/min, fz = 0.1 mm/rev · tooth, and ap = 2.5 mm. This result is due to the fact that despite of milling at medium cutting speeds the temperature between the chip and the tool is increased especially when machining in a dry cutting environment, this combined with low values of feed per tooth and depth of cut (small chip cross-sectional area) might decrease the cutting forces producing less tool wear on the tool flank edge. This result agrees with previous researchers results (Ref 4, 7).

The S/N ratio for the diffusion tool wear mechanism shows that the smaller tool wear is presented in trial 25 (V = 950 m/min, fz = 0.1 mm/rev · tooth, and ap = 3.5 mm) and that the thermal fatigue and mechanical fatigue tool wear mechanisms are presented under the same cutting conditions, where the smaller tool wear is obtained when cutting with V = 350 m/min, fz = 0.1 mm/rev · tooth, and ap = 3.5 mm, which corresponds to trial 7. Table 6 shows the results of the optimal combination of cutting parameters for a specific tool wear mechanism based on the S/N ratio results. Appendix B shows an example of signal-to-noise ratio.

When analyzing this result it can be concluded that in all tool wear mechanisms the smaller tool wear is obtained when using the smaller feed per tooth. Also the different combinations of cutting parameters that are required to obtain a specific tool wear mechanism with exception of thermal and mechanical

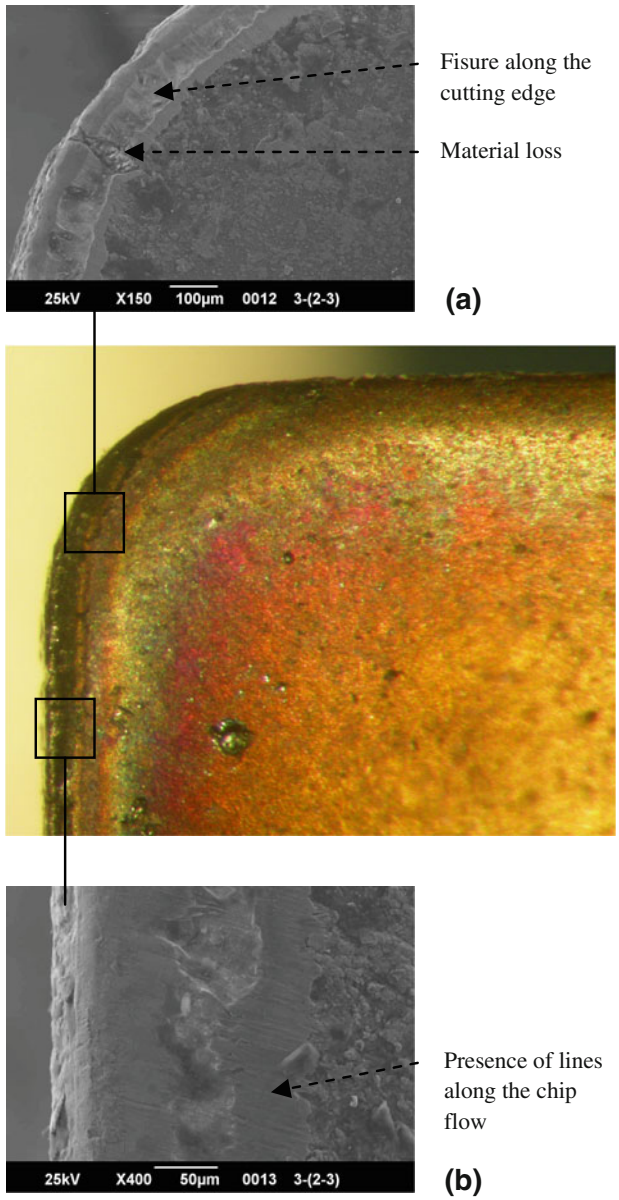

Fig. 6 SEM pictures of different areas of tool's upper face when face milling AISI 1045 with V = 450 m/min, fz = 0.3 mm/rev · tooth, and ap = 3.5 mm. (a) Tool surface with thermal and mechanical fatigue tool wear mechanism, 150× and (b) tool surface with abrasion wear mechanism, 400×

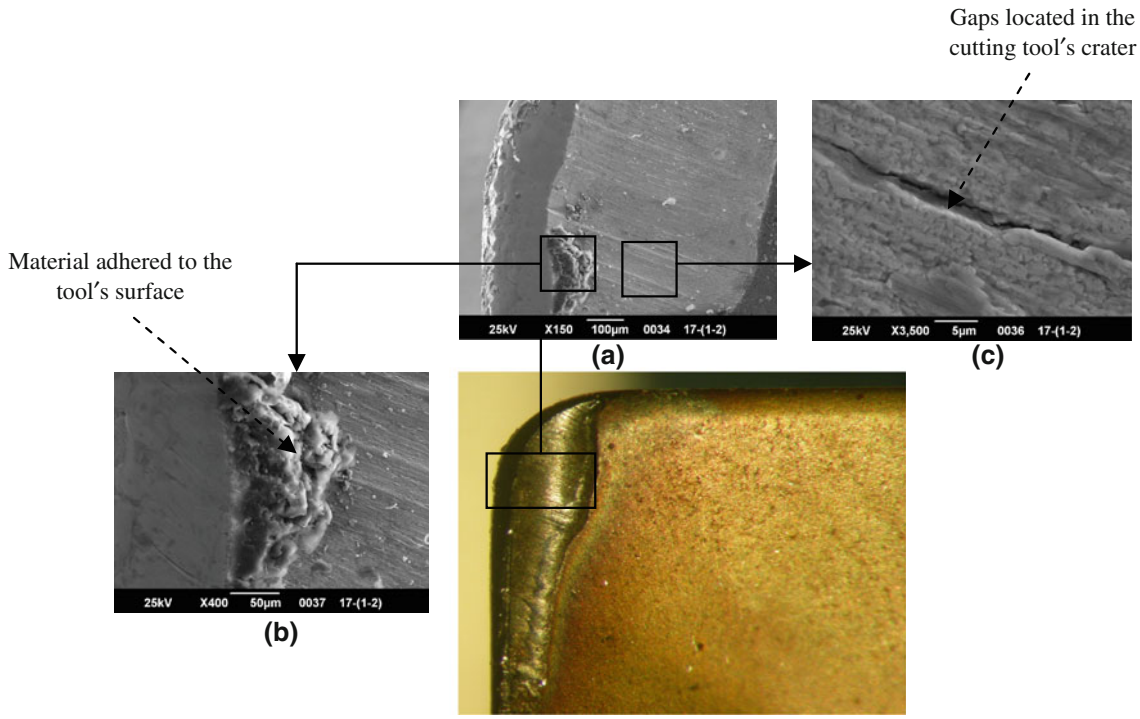

Fig. 7 SEM pictures of different areas of the tool's upper face when face milling AISI 1045 at V = 950 m/min, fz = 0.3 mm/rev·tooth, and ap = 2.5 mm. (a) Tool's surface showing abrasion, diffusion, and adhesion tool wear, 150×, (b) tool's surface showing adhesion tool wear, 400×, and (c) tool's surface showing diffusion tool wear, 3.500×

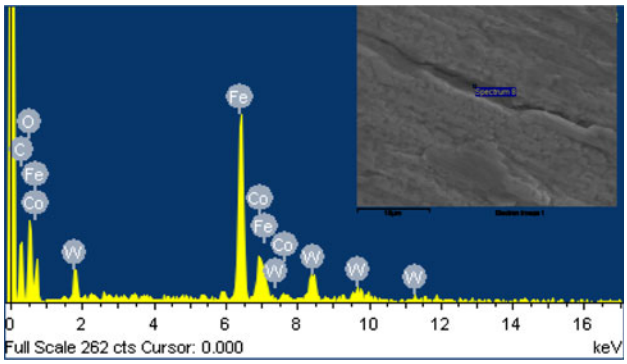

Fig. 8 EDX results of the tool's surface with presence of diffusion tool wear mechanism when face milling AISI 1045

fatigue tool wear mechanism where the same combination of cutting parameters are required. Also it can be observed that the diffusion tool wear mechanism is the one that presented the smaller S/N VB, when compared with the other tool wear mechanism. So it can be concluded that this is the tool wear mechanism that produces more tool flank deterioration when face milling AISI 1045.

In Appendix A, Table 13 and 14 shows the results of tool wear mechanisms under different cutting conditions.

In order to obtain the optimal combination of cutting parameter for a minimum tool wear the individual influence of each cutting parameter on the tool wear was analyzed. Table 7 reports the results.

Once the tool wear results were obtained, the empirical expressions were developed and to secure a good performance of them the Tchebysheff theorem was applied, considering $K = 2$ for each tool wear mechanism, to warranty that 75% of the experimental data is between $\mu \pm 2S$ (μ: media and S: standard deviation). The results are shown in Fig. 10.

As observed from Fig. 10, only one trial was outside the interval and it belongs to the abrasion tool wear mechanism. After analyzing the results the empirical mathematical expressions were developed as a function of the cutting parameters. These expressions were developed using the multiple linear regression by using the Minitab 14 statistical design software. Different adjustments were studied (lineal, exponential, and potential). In this case, the potential adjustment achieved the best result since the multiple correlation coefficient (R^2) and the adjust determination coefficient (R^2_{adj}) were closer to 100% and close to each other and the standard deviation (S) was close to zero (Ref 18). Table 8 shows the results.

As observed from Table 8, R^2 and R^2_{adj} are very high and close to each other, indicating a good tool flank wear adjustment. Also the difference between these two values is 2% indicating a good confidence in the results. The standard deviation (S) is close to zero, indicating that the predicted values are close to the experimental values. The Pearson coefficient (R) shows that the independent variables have a great influence on the tool flank wear under the studied established conditions.

From these relationships it can be observed that the cutting parameters with most influence on the tool flank wear for all the tool wear mechanism is the cutting speed, followed by the feed per tooth and finally the axial depth of cut.

With the idea of validating these expressions, new experiences were conducted. For this case, ten new combinations of cutting parameters were selected to obtain the presence of

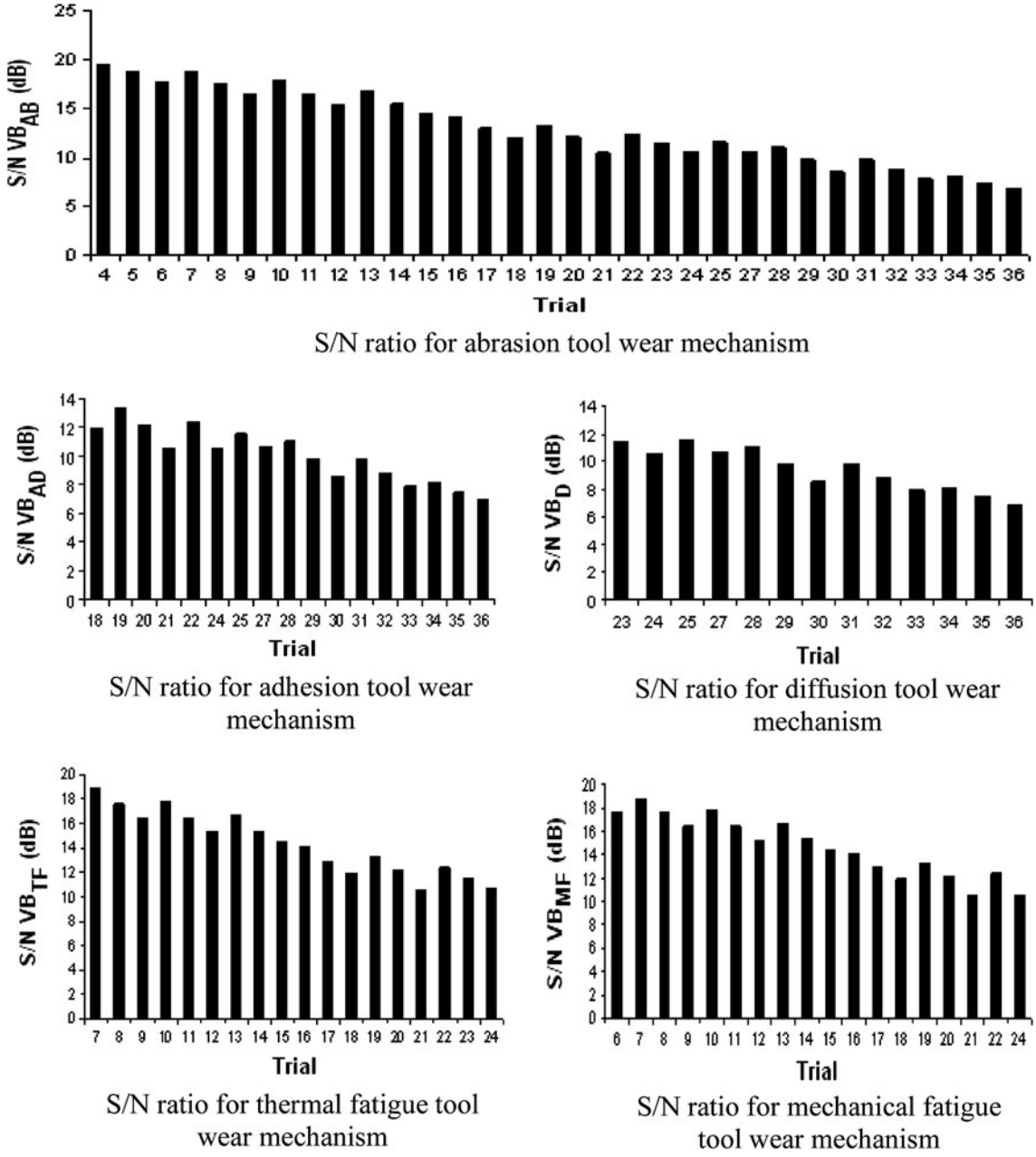

Fig. 9 S/N ratio of each trial for different tool wear mechanisms when face milling AISI 1045

Table 6 Optimal combination of cutting parameters for a smaller tool wear mechanism when face milling AISI 1045

Tool wear mechanism	*V*, m/min	fz, mm/rev · tooth	ap, mm	S/N VB
Abrasion	250	0.1	2.5	19.42
Adhesion	750	0.1	2.5	13.30
Diffusion	950	0.1	3.5	11.58
Thermal fatigue	350	0.1	3.5	18.85
Mechanical fatigue	350	0.1	3.5	18.85

Table 7 Optimal combination of cutting parameters for optimal tool performance (small tool wear) when face milling AISI 1045

Tool wear mechanism	V, m/min	fz, mm/rev · tooth	ap, mm
Abrasion	250	0.1	3.5
Adhesion	550	0.1	2.5
Diffusion	950	0.1	3.5
Thermal fatigue	350	0.1	3.5
Mechanical fatigue	250	0.1	3.5

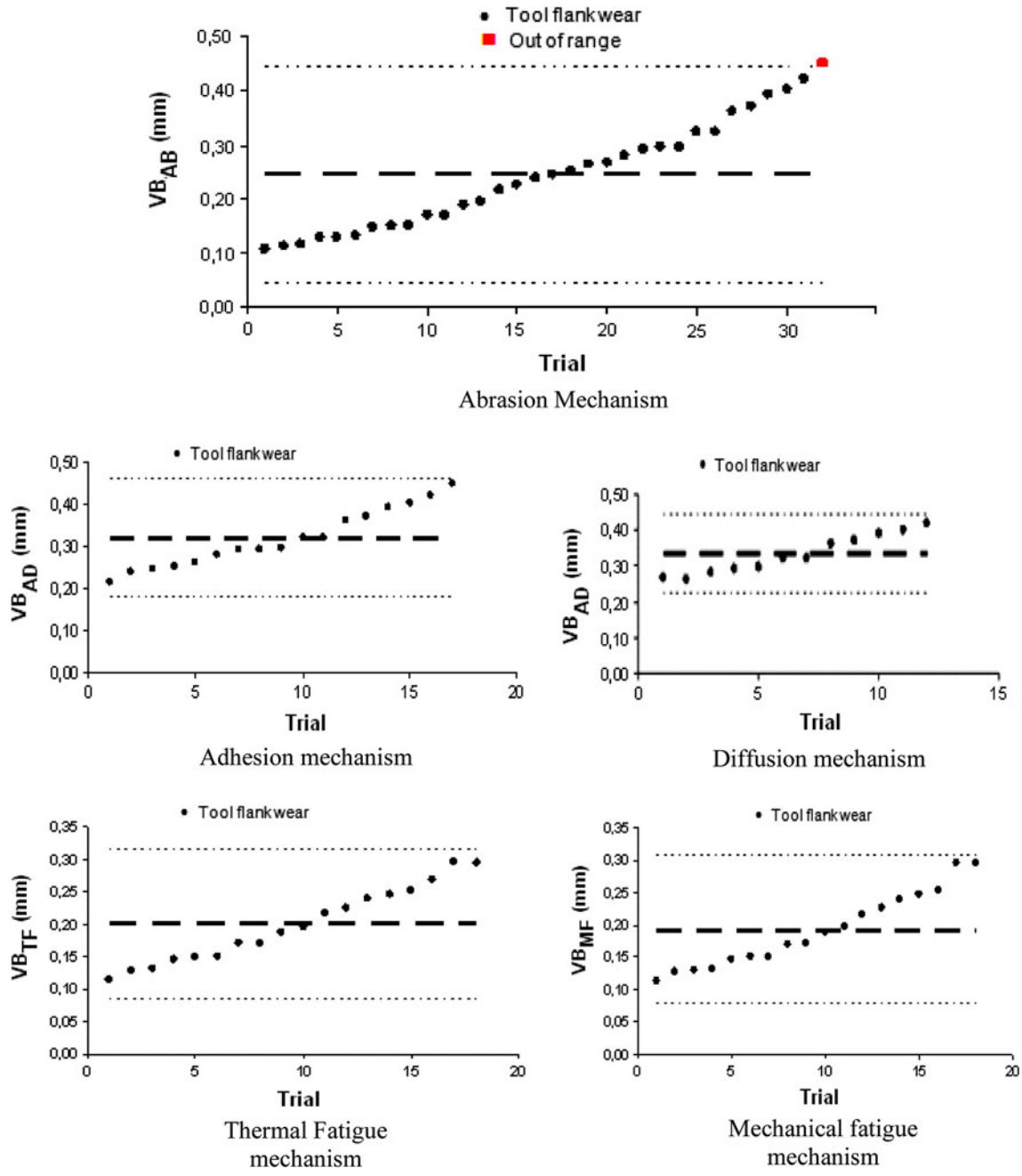

Fig. 10 Tchebysheff theorem for different tool wear mechanisms when face milling AISI 1045

Table 8 Empirical expression for tool flank wear mechanism when face milling AISI 1045

$VB_{AB} = 4.90 \times 10^{-4} \cdot V^{0.8} \cdot fz^{0.14} \cdot ap^{-0.01}$	Eq 3
$R = 97.8\%$, $R^2 = 95.6\%$, $R^2_{adj} = 95.1\%$, $S = 0.04\%$	
$VB_{AD} = 1.66 \times 10^{-4} \cdot V^{0.96} \cdot fz^{0.14} \cdot ap^{0.09}$	Eq 4
$R = 96.2\%$, $R^2 = 92.6\%$, $R^2_{adj} = 91.0\%$, $S = 0.03\%$	
$VB_{D} = 2.34 \times 10^{-5} \cdot V^{1.24} \cdot fz^{0.13} \cdot ap^{0.07}$	Eq 5
$R = 96.7\%$, $R^2 = 93.6\%$, $R^2_{adj} = 91.7\%$, $S = 0.02\%$	
$VB_{TF} = 2.69 \times 10^{-4} \cdot V^{0.87} \cdot fz^{0.16} \cdot ap^{-0.004}$	Eq 6
$R = 98.0\%$, $R^2 = 96.0\%$, $R^2_{adj} = 95.2\%$, $S = 0.03\%$	
$VB_{MF} = 3.72 \times 10^{-4} \cdot V^{0.8} \cdot fz^{0.18} \cdot ap^{-0.03}$	Eq 7
$R = 97.1\%$, $R^2 = 94.3\%$, $R^2_{adj} = 93.1\%$, $S = 0.04\%$	

different tool wear mechanisms. Table 9 shows the new selected cutting parameters.

The models were validated to evaluate the efficiency and the ability of them to predict the tool flank wear (VB_p), the $\%RE_p$ (predictive relative error percentage) criterion was used, as defined in Eq 1

$$\%RE_p = \left|\frac{VB - VB_p}{VB}\right| * 100 \quad \text{(Eq 1)}$$

where VB is the experimental tool flank wear (mm) and VB_p is the predictive tool flank wear (mm).

These results are shown in Table 10 and 11.

As observed from Table 10 and 11, the experimental and predictive values of tool wear are similar and the average

Table 9 New combination of cutting parameters for the validation of the developed empirical expressions for different tool wear predictions

	Cutting parameter		
Trial	*V*, m/min	fz, mm/rev · tooth	ap, mm
1	250	0.3	4.0
2	450	0.2	2.5
3	550	0.2	4.0
4	650	0.1	4.0
5	850	0.3	4.0
6	950	0.1	3.5
7	1050	0.1	2.5
8	1050	0.2	2.5
9	1150	0.2	4.0

Table 10 Experimental and predictive values of tool flank wear when face milling AISI 1045, for abrasion (AB), adhesion (AD), and diffusion (D) tool wear mechanism and their respective predictive relative error

	Experimental	Predictive, mm			$\%RE_p$		
Trial	VB	$VB_{p_{AB}}$	$VB_{p_{AD}}$	VB_{p_D}	$\%RE_{p_{AB}}$	$\%RE_{p_{AD}}$	$\%RE_{p_D}$
1	0.08	0.08	…	…	0.00	…	…
2	0.15	0.14	…	…	6.67	…	…
3	0.17	0.17	…	…	0.00	…	…
4	0.20	0.18	0.17	…	10.00	15.00	…
5	0.29	0.33	0.32	0.22	13.79	10.34	24.14
6	0.27	0.28	0.28	0.20	3.70	3.70	25.93
7	0.28	0.32	0.32	0.23	14.29	14.29	21.43
8	0.32	0.36	0.35	0.26	12.50	9.37	18.75
9	0.33	0.39	0.40	0.29	18.18	24.24	12.12
				% RE_p^*	8.19	12.83	20.47

Table 11 Experimental and predictive values of tool flank wear values when face milling AISI 1045, for mechanical fatigue (MF) and thermal fatigue (TF) tool wear mechanism and their respective relative error

	Experimental	Predictive, mm		$\%RE_p$	
Trial	VB	$VB_{p_{MF}}$	$VB_{p_{TF}}$	$\%RE_{p_{MF}}$	$\%RE_{p_{TF}}$
1	0.08	0.07	0.08	5.88	0.00
2	0.15	…	0.15	…	0.00
3	0.17	0.16	0.18	5.88	5.88
4	0.20	0.18	0.20	10.00	0.00
5	0.29	…	0.36	…	24.14
6	0.27	…	0.33	…	22.22
7	0.28	0.33	…	17.86	…
8	0.32	0.40	…	25.00	…
9	0.33	…	…	…	…
			% RE_p^*	12.92	8.71

relative error for the abrasion, adhesion, and diffusion tool wear mechanism is 8, 13, and 20%, respectively, and for the mechanical fatigue and thermal fatigue tool wear mechanism is 13 and 9%, respectively. This error can be considered as a good approximation considering that the resolution of the tool microscope used to measure the tool flank wear is 0.01 mm.

With regard to the critical cutting speed (V^*, the speed value where the diffusion tool wear mechanism starts to appears) for the milling of AISI 1045 the results show that this value is $V^* = 850$ m/min and the range of critical cutting speed is between 850 and 1250 m/min.

The tool wear results corresponding to the diffusion tool wear mechanism are employed for the development of the critical cutting speed prediction model. This relationship is developed applying a multiple linear regression method where the independent variables are the feed per tooth (fz), the axial depth of cut (ap), and the cutting time (t). Different adjustments were studied (linear, potential, and exponential) selecting the one that fulfills all the statistical variables. Equation 2 shows the developed model.

$$V_p^* = 5.75 \times 10^4 \cdot \mathrm{fz}^{-0.75} \cdot \mathrm{ap}^{-0.15} \cdot t^{-0.68}$$
$$R = 95.81\%,\ R^2 = 91.8\%,\ R^2_{\mathrm{adj}} = 88.7\%,\ S = 0.02\%. \quad \text{(Eq 2)}$$

As observed from Eq 2, the feed per tooth is the variable with most influence on the critical cutting speed, followed by the cutting time and finally the axial depth of cut. The influence of the feed per tooth on the critical cutting speed is probably due to the fact that as the feed per tooth is decreased, the chip cross-sectional area is also decreased generating less cutting forces as well as a lower temperature in the tool-workpiece interface, decreasing the time for the diffusion tool wear mechanism to appear.

The model for critical cutting speed was also validated. In this case, five new trials were conducted and Table 12 shows the results.

5. Conclusions

- The developed expressions make a new and valuable contribution to the metalworking industry by predicting the tool wear for different tool wear mechanisms and the critical cutting speed when face milling AISI 1045 with an accuracy of 92% for the abrasion mechanism, 87% for the adhesion mechanism, 80% for the diffusion mechanism, 87% for the mechanical fatigue mechanism, and 91% for the thermal mechanism. For the critical cutting speed the accuracy is of 96%.
- The feed per tooth has the most influence on the critical cutting speed, followed by the cutting time and finally the axial depth of cut.
- The ranges of cutting speed to obtain the abrasion tool wear mechanism is 250-1250 m/min, for the adhesion mechanism is 650-1250 m/min, the diffusion mechanism is 850-1250 m/min, the mechanical fatigue mechanism is 350-850 m/min, and for the thermal fatigue mechanism is 250-850 m/min.
- Under the selected cutting conditions, the cutting tool is affected by the abrasion, adhesion, diffusion, mechanical, and thermal fatigue mechanisms when face milling AISI 1045.
- The cutting speed is the parameter with most influence on the tool flank wear, followed by the feed per tooth and finally with the axial depth of cut.

Table 12 Experimental (V_e^*) and predictive (V_p^*) values of critical cutting speed when face milling AISI 1045 using Eq 2

Trial	fz, mm/rev · tooth	ap, mm	*t*, s	V_e^*, m/min	(V_p^*), m/min	%RE_p
1	0.3	4.0	0.12	850	872	2.59
2	0.1	3.5	0.58	950	996	4.83
3	0.1	4.0	0.58	1050	976	7.03
4	0.2	2.5	0.29	1050	998	4.98
5	0.2	4.0	0.21	1150	1092	0.22
					% RE_p^*	3.93

Table 13 Wear mechanisms obtained for Group 1 when face milling 1045 steel under different cutting conditions

				Wear mechanism					
Trial	*V*, m/min	fz, mm/rev · tooth	ap, mm	Abrasion	Adhesion	Diffusion	Thermal fatigue	Mechanical fatigue	VB, mm
1	150	0.1	2.5	X					
2	150	0.2	3.5	X					
3	150	0.3	4.0	X					
4	250	0.1	2.5	X			X	X	0.107
5	250	0.2	3.5	X					0.116
6	250	0.3	4.0	X			X	X	0.131
7	350	0.1	3.5	X			X	X	0.114
8	350	0.2	4.0	X			X	X	0.132
9	350	0.3	2.5	X			X	X	0.150
10	450	0.1	4.0	X			X	X	0.128
11	450	0.2	2.5	X			X	X	0.150
12	450	0.3	3.5	X			X	X	0.171
13	550	0.1	3.5	X			X	X	0.147
14	550	0.2	4.0	X			X	X	0.170
15	550	0.3	2.5	X	X		X	X	0.188
16	650	0.1	4.0	X	X		X	X	0.197
17	650	0.2	2.5	X	X				0.226
18	650	0.3	3.5	X			X		0.253

X, a tool wear mechanism

Table 14 Wear mechanisms obtained for Group 2 when face milling 1045 steel under different cutting conditions

				Wear mechanism					
Trial	*V*, m/min	fz, mm/rev · tooth	ap, mm	Abrasion	Adhesion	Diffusion	Thermal fatigue	Mechanical fatigue	VB, mm
1	750	0.1	2.5	X	X			X	0.216
2	750	0.2	3.5	X			X		0.247
3	750	0.3	4.0	X	X	X	X	X	0.297
4	850	0.1	2.5	X			X	X	0.240
5	850	0.2	3.5	X					0.268
6	850	0.3	4.0	X	X	X	X		0.295
7	950	0.1	3.5	X	X	X			0.264
8	950	0.2	4.0	Tool failed					
9	950	0.3	2.5	X	X	X			0.294
10	1050	0.1	4.0	X	X	X		X	0.280
11	1050	0.2	2.5	X	X	X		X	0.322
12	1050	0.3	3.5	X	X	X			0.372
13	1050	0.1	4.0	X	X	X			0.323
14	1150	0.2	4.0	X	X	X			0.362
15	1150	0.3	2.5	X	X	X			0.403
16	1250	0.1	4.0	X	X	X			0.393
17	1250	0.2	2.5	X	X	X		X	0.423
18	1250	0.3	3.5	X	X	X			0.451

X, a tool wear mechanism

Appendix A

The results of tool wear mechanisms for Groups 1 and 2 under different cutting conditions are shown in Table 13 and 14.

Appendix B: Signal-to-Noise Ratio Example

As previously stated the ''smaller-the-best'' statistical measure of performance, called signal-to-noise ratio (S/N), developed by Taguchi was applied. The formula is as follow:

$$S/N = -10\log(VB)^2 \quad \text{(Eq 8)}$$

From Table 10 it is observed that $VB_{AB} = 0.17$ mm for Trial 4. Substituting this value in Eq 8, it is obtained that S/N_{ratio} $VB_{AB} = 15.39$ dB

References

1. M.A. Elbestawi, L. Chen, C.E. Becze, and T.I. El-Wardany, High-Speed Milling of Dies and Molds in their Hardened State, *Ann. CIRP*, 1997, **46**(1), p 57–62
2. P. Koshy, R.C. Dewes, and D.K. Aspinwall, High Speed End Milling of Hardened AISI, D2 Tool Steel (58 HRc), *J. Mater. Process. Technol.*, 2002, **127**, p 266–273
3. S. Hogmark, *Wear Mechanisms of HSS Cutting Tools*, Uppsala University, Uppsala, 2001
4. Z.Q. Liu, X. Ai, H. Zhang, Z.T. Wang, and Y. Wan, Wear Patterns and Mechanisms of Cutting Tools in High-Speed Face Milling, *J. Mater. Process. Technol.*, 2002, **129**, p 222–226
5. Z. Cassier, Y. Prato, and P. Muñoz-Escalona, Built-Up Edge Effect on Tool Wear when Turning Steels at Low Cutting Speed, *J. Mater. Eng. Perform.*, 2004, **13**(5), p 542–547
6. A. Devillez, S. Lesko, and W. Mozer, Cutting Tool Crater Wear Measurement with White Light Interferometry, *Wear*, 2003, **256**, p 56–65
7. K. Serdar, A. Adem, U. Mustafa, and O. Bilgehan, Effect of Cutting Speed on Tool Performance in Milling of B4CP Reinforced Aluminum Metal Matrix Composites, *J. Mater. Process. Technol.*, 2006, **178**, p 241–246
8. A.C. De Melo, J.C. Milan, M.B. Da Silva, and A. Machado, Some Observations on Wear and Damages in Cemented Carbide Tools, *J. Braz. Soc. Mech. Sci. Eng.*, 2006, **XXVIII**(3), p 269–277
9. T.L. Banh, Q.T. Phan, and D.B. Nguyen, Wear Mechanisms of PDV Coated HSS End Mills Used to Machine 1045 Hardened Steel, *J. Mater.*, 2005, **1**, p 1–12
10. A. Molinari and M. Nouari, Modelling of Tool Wear by Diffusion in Metal Cutting, *Wear*, 2000, **252**, p 135–149
11. S.K. Choudhury and P. Srinivas, Tool Wear Prediction in Turning, *J. Mater. Process. Technol.*, 2004, **153–154**, p 276–280
12. I. Korkut, M. Kasap, I. Ciftc, and U. Seker, Determination of Optimum Cutting Parameters During Machining of AISI, 304 Austenitic Stainless Steel, *Mater. Des.*, 2004, **25**, p 303–305
13. B. Gopalsamy, B. Mondal, and S. Ghosh, Taguchi Method and ANOVA: An Approach for Process Parameters Optimization of Hard Machining while Machining Hardened Steel, *J. Sci. Ind. Res.*, 2009, **68**, p 686–695
14. M. Calamaz, J. Limido, M. Nouari, C. Espinosa, D. Coupard, M. Salaun, F. Girot, and R. Chieragatti, Toward a Better Understanding of Tool Wear Effect Trough a Comparison Between Experiments and SPH Numerical Modelling of Machining Hard Materials, *Int. J. Refract. Met. Hard Met.*, 2009, **27**(3), p 595–604
15. F. Rashed and T. Makmoud, Prediction of Wear Behaviour of A356/SiCpMMCs Using Neural Networks, *Tribol. Int.*, 2009, **42**(5), p 642–648
16. ISO 8688-1 Tool, Life Testing in Milling Part 1: Face Milling, 1st ed., 1989, p 1–27
17. S. Coromant, *Modern Metal Cutting*, Tofters Tryckeri AB, Sandviken, 1994
18. D.C. Montgomery, *Design Analyses of Experiments*, 3rd ed., Wiley, New York, 1997